MACHINE LEARNING-BASED SWITCH CIRCUIT POSITIONING FOR SINGLE-ELEMENT SWITCHED-BEAM ANTENNA

Pichaya Chaipanya[1*], Kanyapat Sangchan[1], Worakan Noimi[1], Korawit Pachuen[1], Samran Santalunai[2], and Nuchanart Santalunai[3]

[1]Department of Electrical Engineering, Faculty of Engineering, Srinakharinwirot University, Ongkharak, Nakhon Nayok 26120, Thailand

[2]School of Electronic Engineering, Institute of Engineering, Suranaree University of Technology, Nakhon Ratchasima 30000, Thailand

[3]Department of Telecommunication Engineering, Faculty of Engineering and Technology, Rajamangala University of Technology Isan, Nakhon Ratchasima 30000, Thailand

*Corresponding Author.
E-mail address: pichayac@g.swu.ac.th

ABSTRACT

This paper presents the design, fabrication, and performance evaluation of a 2.6 GHz switched beam antenna for 5G applications, incorporating machine learning techniques for beam direction and return loss prediction. The antenna, a single circular microstrip patch, is capable of beam switching in eight directions (0º, 45º, 90º, 135º, 180º, 225º, 270º, and 315º) by implementing short circuits at specific terminal edges controlled by a microcontroller. The input parameters for machine learning include the distance between short circuit points, the number and direction of short circuit holes, and their radial position from the antenna center. A dataset of 148 samples was generated using CST Studio Suite simulations, and four machine learning algorithms—Gradient Regression, Lasso Regression, Linear Regression, and Random Forest—were applied to predict the main beam direction and return loss. The predictions were compared with CST results, and among the tested algorithms, Random Forest demonstrated the highest accuracy. Subsequently, the antenna was fabricated and experimentally measured, with results confirming beam steering capabilities and a maximum gain of 11 dBi. The measured performance was further compared with both CST simulations and machine learning predictions, validating the effectiveness of the proposed approach in accurately predicting antenna characteristics.

KEYWORDS: Antenna, Switched beam, Shorted circuit, Machine Learning, Artificial Intelligence.

1. INTRODUCTION

In the era of 5th Generation (5G) wireless communication [1-5], the demand for high-speed, high-quality, and reliable connectivity has significantly increased. Wireless communication plays a crucial role in various applications, including telecommunications, healthcare, and remote communication. As the population grows and the need for seamless connectivity expands to diverse environments, including remote and urban areas, antenna technology continues to evolve to meet these demands. Modern antennas are designed to be smaller, cost-effective, and capable of efficiently directing signals to desired locations while minimizing interference.

A critical challenge in wireless communication is the unwanted propagation of signals, which can lead to interference and reduced system efficiency. To address this, beam-switching antennas [6-7] have gained attention, as they can dynamically steer their main lobe toward desired directions while suppressing side lobes or null in undesired directions. This improves signal quality and system performance. Among various antenna types, directional antennas are particularly useful for point-to-point communication, as they offer higher gain and longer transmission distances compared to omnidirectional antennas. The beam-switching technique further enhances their performance by providing adaptive signal directionality, which is essential in 5G networks.

Several works have demonstrated the effectiveness of single-element switched-beam antennas in improving wireless communication by dynamically steering beams while minimizing interference. For instance, [8-9] introduced a low-cost, multiband switched beam antenna designed for 5G applications. Their design enables beam switching across multiple frequency bands, improving signal coverage and network efficiency without requiring complex phased array systems. Further advancements in single-element antenna design have focused on performance improvements. Reducing backlobe radiation in a circular patch antenna [10], which helps enhance radiation efficiency. Next, the work [11] developed a compact antipodal Vivaldi antenna with consistent gain, suitable for 5G communication. Additionally, the work [12] explored the use of shorting pins in microstrip patch antennas to reduce the specific absorption rate (SAR), ensuring better safety and efficiency in mobile applications.

One of the widely explored approaches for improving beam-switching antenna performance is the integration of Machine Learning (ML) techniques. Antenna design involves numerous complex parameters, making it challenging to optimize performance manually. ML algorithms can analyze large datasets and identify optimal configurations, reducing design complexity and computation time while improving accuracy and efficiency. Several research efforts have successfully implemented ML-based techniques for antenna optimization, achieving significant improvements in gain such as the work presented in [13], designed and optimized a rectangular patch antenna at 28 GHz, demonstrating how different substrate materials significantly affect gain, efficiency, and directivity. By employing a Multivariate Polynomial Regression (MPR) model, the study effectively predicted antenna parameters with high accuracy ($R^2 = 0.9999$), eliminating the need for extensive physical prototyping and accelerating the design process. The work presented in [14] reviewed various ML algorithms applied to optimize antenna parameters, including gain, bandwidth, and radiation patterns, demonstrating the effectiveness of ML in enhancing antenna performance. Similarly, [15] developed a high-gain, low-return-loss Quasi-Yagi–Uda antenna operating at 3.5 GHz for the n78 band of 5G. The paper utilized supervised regression ML models, where Linear Regression provided the best prediction for resonant frequency, and Gaussian Process Regression demonstrated superior performance for gain prediction, achieving an accuracy close to 99%. The paper highlights the potential of ML techniques in enhancing antenna gain while reducing design complexity and time. Moreover, work [16-17] introduced a machine learning-based generative method that automates antenna design and optimization by employing a flexible geometric scheme based on a mesh network. The method integrates discriminators and generators to predict and generate optimal antenna geometries, improving the efficiency of the design process. Their approach, when applied to a dual resonance antenna with wide bandwidth, performed comparably to the Trust Region Framework and outperformed other conventional ML algorithms such as Genetic Algorithm (GA) and Particle Swarm Optimization (PSO). In addition, the study [18] utilized machine learning techniques to enhance the gain and resonance performance of Quasi-Yagi–Uda antennas. The research found that the Linear Regression and Gaussian Process Regression algorithms provided the most accurate predictions for optimizing antenna performance.

In terms of return loss prediction, machine learning has been applied to enhance the efficiency of antenna design and optimization. For example, the review paper [19] provides a comprehensive overview of how ML and DL techniques contribute to antenna engineering. The study highlights the role of electromagnetic (EM) simulators such as CST and HFSS in generating datasets for ML-based return loss prediction. Various optimization strategies, including surrogate-based and multi-objective optimization, are explored to refine antenna performance parameters such as return loss. In addition, [20] explores the use of regression-based ML techniques to predict resonant frequency and optimize the dimensions of a compact microstrip antenna (SPCMA). The research utilizes CST Microwave Studio to simulate 3,822 antenna variations by adjusting slot size, material thickness, patch length, and dielectric properties across multiple frequency bands. Next, the work presented in [21] employed seven ML models, including Convolutional Neural Network (CNN), Linear Regression, Random Forest Regression (RFR), Decision Tree Regression (DTR), and Extreme Gradient Boosting (XGB), to estimate the resonance frequency of patch antennas. The Decision Tree Regression model yielded the best results, with an R-squared score of 99.68%. Similarly, the work presented in [22] applied ML techniques to predict the return loss (S_{11}) of microstrip patch antennas. The study compared Decision Tree, Random Forest, XGBoost, and KNN models, with KNN exhibiting the most accurate predictions.

Next, improvements in beam direction control using ML have been explored in various works, such as the work on hybrid plasmonic nano-antenna arrays [23], where deep neural networks (DNN) and optimization techniques were employed for precise beam steering. In this work, different beam-steering techniques, including switched-beam and phased-array approaches, were investigated. The authors proposed a hybrid method that utilizes a neural network to predict the appropriate feeding phases of antenna elements, enhancing beam-steering accuracy. Additionally, a weighted hybrid gravitational search algorithm combined with particle swarm optimization was used to further refine the beam-steering process, demonstrating the effectiveness of ML in optimizing beam direction control. Furthermore, deep neural networks (DNNs) have been employed to enhance beam steering capabilities in antenna arrays [24]. A study implemented a DNN-based approach for beam-steering control in a uniform circular antenna array, optimizing the main beam direction while maintaining a side-lobe level of ≤ -30 dB. Using a hybrid optimization algorithm combining particle swarm optimization (PSO) and a modified gravitational search algorithm (MGSA-PSO), the model accurately estimated the appropriate feeding phases of the 16 antenna elements. The experimental results demonstrated the effectiveness of the DNN-based approach in dynamically steering the beam pattern toward desired directions, improving directional control in 5G applications. Moreover, a study in beam prediction through machine learning focuses on the evaluation of beam-steering in a metasurface-based terahertz (THz) antenna for 6G networks [25]. This research employs a machine learning approach to assess the radiation pattern of a photoconductive THz antenna loaded with a graphene-based digital metasurface (MSF). The metasurface, consisting of graphene meta-atoms, enables reconfigurable beam-steering by switching the meta-atom states between ON and OFF to generate specific beam directions. The machine learning model helps characterize the antenna's radiation pattern with greater speed and accuracy, avoiding the need for computationally intensive full-wave simulations. Among five machine learning models tested, the Extreme Randomized Tree algorithm provided the most accurate predictions, with an R-squared score of 0.9966. While most machine learning applications in beam steering focus on antenna arrays, where algorithms calculate weights or phase shifts for each element, there is increasing interest in ML-driven techniques for single-element switched-beam antennas. These antennas offer a more compact and simplified solution for beamforming while benefiting from predictive modeling. For example, a study on a wideband circular slot antenna utilized ML algorithms to predict beam-switching directions based on key parameters, including the distance from the center, shorted circuit positions, and the number of shorting points [26]. The study compared five ML algorithms and found that Decision Trees and Random Forest provided the most accurate predictions. Similarly, another study on ultra-wideband spiral antennas applied ML techniques to predict beam-switching directions by analyzing slot positions and the turn number of the ring [27]. Using a dataset of 200 simulated configurations, the researchers evaluated Decision Trees, Random Forest, and K-Nearest Neighbors (KNN), with Decision Trees and Random Forest delivering the highest prediction accuracy. These works highlight the potential of ML in optimizing beam switching for compact, single-element antennas, making them promising solutions for efficient and adaptive beamforming in 5G applications.

This paper presents the design, simulation, fabrication, and testing of a 2.6 GHz single circular microstrip switched-beam antenna for 5G applications. The antenna can steer its beam in eight directions (0º, 45º, 90º, 135º, 180º, 225º, 270º, and 315º) by implementing short circuits at specific terminal edges, controlled by a microcontroller. To enhance the design process, ML techniques are applied to predict both the main beam direction and return loss using a dataset generated from CST Studio Suite simulations. Four ML algorithms—Gradient Regression, Lasso Regression, Linear Regression, and Random Forest—are utilized, and their predictive performance is evaluated by comparing the results with CST simulations. The most effective ML model is then identified. Finally, the antenna is fabricated, and its performance is measured to validate the ML predictions and simulation results.

By integrating ML into the beam-switching antenna design, this study achieves two key objectives: (1) predicting the return loss at 2.6 GHz to optimize impedance matching and overall performance, and (2) forecasting the main beam direction based on variations in shorted positions and the number of shorted circuit holes, enabling efficient beam control. These capabilities enhance the adaptability and accuracy of switched-beam antennas, supporting the advancement of smart antenna systems for future 5G networks.

The rest of the paper is structured as follows: Section 2 describes the design of the 2.6 GHz circular microstrip antenna and the implementation of the switched-beam mechanism. Section 3 presents the application of machine learning techniques for predicting return loss and beam directions based on variations in input parameters. Section 4 discusses the experimental validation of the fabricated antenna, comparing measured results with CST simulations and ML predictions. Finally, Section 5 provides the conclusion.

2. ANTENNA DESIGN AND SWITCHED-BEAM IMPLEMENTATION

To develop an efficient beam-switching antenna for 5G applications, a circular microstrip patch antenna operating at 2.6 GHz is designed. This frequency is one of the allocated bands for 5G in Thailand, making it suitable for wireless communication applications. The antenna is optimized to achieve a well-matched impedance, ensuring minimal return loss and stable performance.

To enable beam switching, a systematic approach is employed where short circuits are introduced at specific locations along the antenna's perimeter. These short circuits dynamically alter the current distribution, allowing the main beam to steer in predefined directions. This section details the design principles, simulation setup, and beam-switching mechanism used to achieve directional control.

2.1 DESIGN OF THE 2.6 GHZ CIRCULAR MICROSTRIP ANTENNA

The designed single circular microstrip antenna features a substrate with a thickness of 1.6 mm, while both the conductor and ground plane have a thickness of 0.03 mm. The substrate and ground plane dimensions are 150 mm × 150 mm. The antenna is constructed using a dielectric material with a relative permittivity (ε_r) of 4.4. The initial radius of the circular patch, denoted as a, is determined using the formula [28]:

$$a = \frac{F}{\left\{1 \times \frac{2h}{\pi \varepsilon_r F}\left[In\left(\frac{\pi F}{2h}\right) + 1.7726\right]\right\}^{\frac{1}{2}}} \quad (1)$$

where h represents the substrate thickness which F can be obtained from

$$F = \frac{8.791 \times 10^9}{f_r \sqrt{\varepsilon_r}} \quad (2)$$

where f_r is the resonant frequency, set at 2.6 GHz. Using these parameters, the calculated initial radius is 15.62 mm.

This initial radius was implemented in CST Studio Suite for simulation; however, the results did not meet the desired performance criteria. To enhance the antenna's performance, the radius was increased to four times its original value, resulting in a new radius of 62.48 mm. Further fine-tuning was performed to optimize the return loss, leading to a final selected radius of 58.5 mm.

The final antenna configuration is illustrated in Figure 1(a), while the radiation pattern and corresponding return loss characteristics are presented in Figure 1(b) and Figure 1(c), respectively.

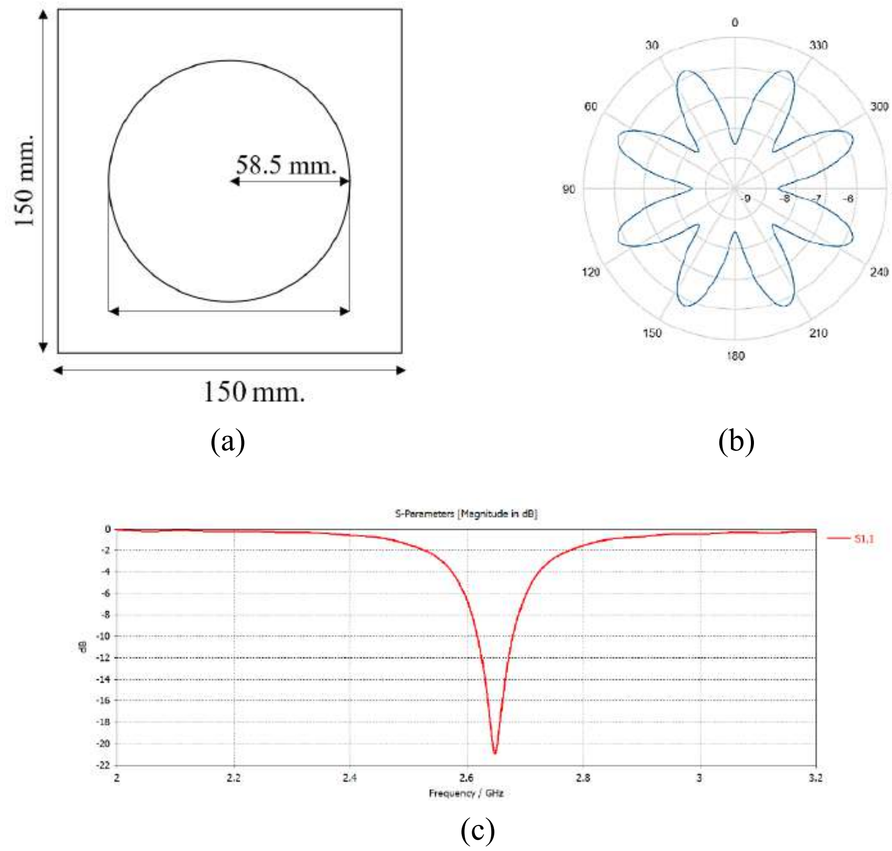

Figure 1. Simulation of circular microstrip patch antenna (a) structure (b) radiation pattern and (c) return loss.

2.2 SWITCHED-BEAM CONFIGURATION AND OPERATING MECHANISM

The antenna is designed with a switched-beam mechanism by introducing short-circuiting holes along the inner edge of the circular patch. These holes are strategically placed at points where the current distribution is minimal, influencing the radiation pattern and altering the current flow across the antenna surface.

Initially, four short-circuiting holes were introduced; however, this configuration failed to achieve beam switching. Subsequently, the number of holes was increased to 8 and then to 16, but beam switching was still not observed. It was only when the number of short-circuiting holes was increased to 32 that beam switching was successfully achieved, enabling the main beam to steer in eight distinct directions, as summarized in Table 1.

Table 1. Configurations and radiation patterns of the antenna with 32 holes.

Case	Antenna configuration	Radiation pattern	Main beam direction
1	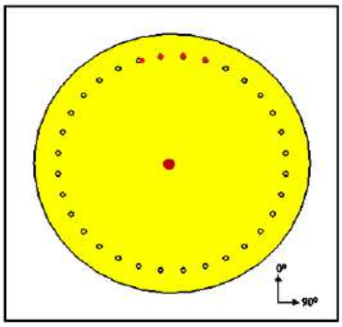	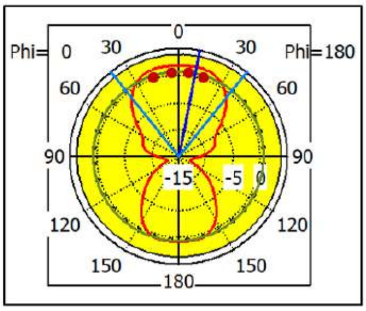	0°
2	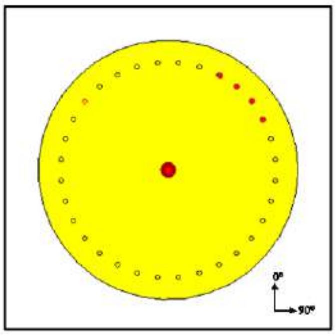	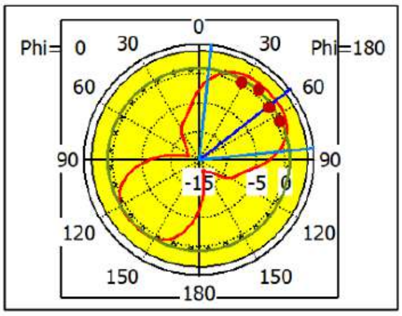	45°
3	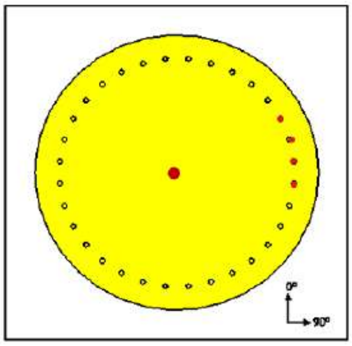	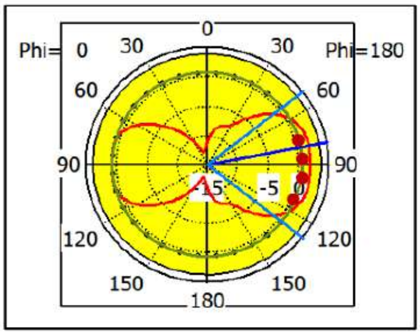	90°
4	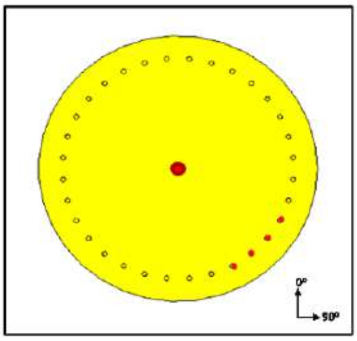	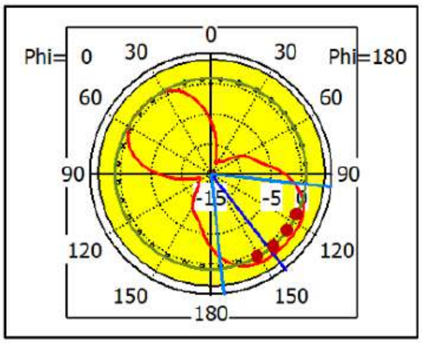	135°

Table 1. Configurations and radiation patterns of the antenna with 32 holes. (Count.)

<table>
<tr><th>Case</th><th>Antenna configuration</th><th>Radiation pattern</th><th>Main beam direction</th></tr>
<tr><td>5</td><td>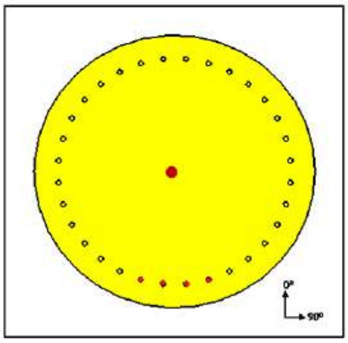
</td><td>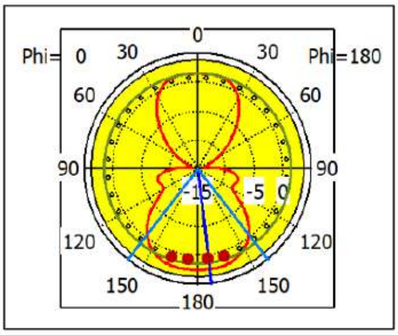
</td><td>180˚</td></tr>
<tr><td>6</td><td>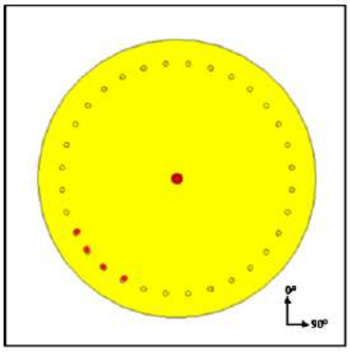
</td><td>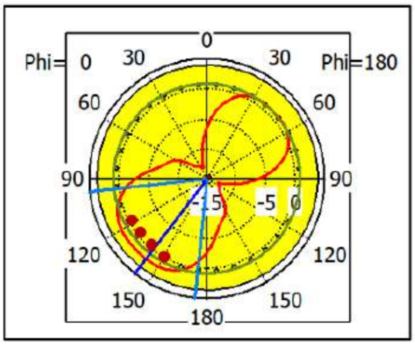
</td><td>225˚</td></tr>
<tr><td>7</td><td>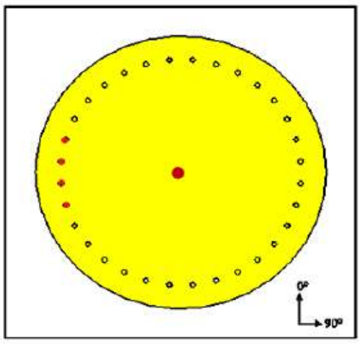
</td><td>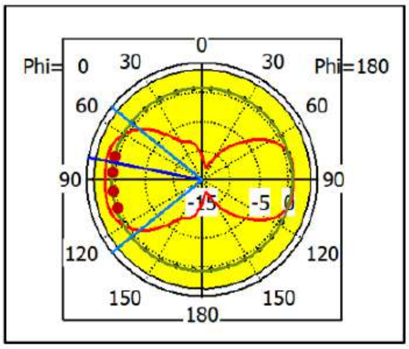
</td><td>270˚</td></tr>
<tr><td>8</td><td>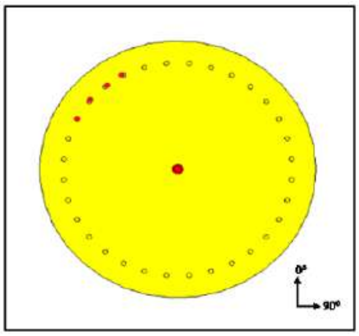
</td><td>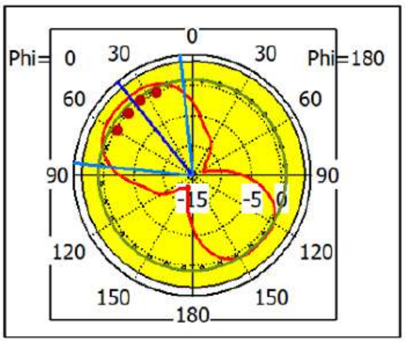
</td><td>315˚</td></tr>
</table>

In Table 1, the red dots represent open circuits, which determine the direction of the main beam. The radiation pattern is primarily directed toward the open circuit regions, as these areas allow for maximum radiation, while the short-circuited points affect the current distribution and steering capability. In this configuration, the antenna includes 32 holes in total, with 28 short-circuited and 4 left as open circuits. These open circuits, indicated by red dots, play a critical role in determining the main beam direction by allowing maximum radiation, while the shorted holes influence the current distribution and enable beam steering. Additionally, as shown in Figure 2, the return loss remains consistent across all eight beam-switching cases in Table 1. This consistency is due to the symmetric structure of the antenna and the uniform distribution of shorted circuits. The antenna operates within the 2.6 GHz frequency band, ranging from 2.573 GHz to 2.62 GHz.

While 32 holes marked the threshold for achieving beam switching, further variations in the number of holes and their spacing improved the antenna's performance. For instance, a configuration with 56 holes, grouped into eight sets of seven holes each, was simulated. Within each group, the holes were evenly spaced, but the spacing between adjacent groups differed from the intra-group spacing, as detailed in Table 2. This configuration resulted in eight distinct short-circuiting cases, each corresponding to a specific main beam direction. Similar to Table 1, Table 2 presents these eight beam-switching configurations using an alternative short-circuiting pattern. The red dots represent the open circuits, which define the direction of the main beam, while the. shorted holes influence the current distribution and facilitate directional control. As shown in Figure 3 shows that the return loss across all eight configurations remains consistently acceptable, confirming that the antenna effectively operates at the desired frequency of 2.6 GHz. This stability is attributed to the symmetrical structure and balanced grouping of the short-circuited positions, ensuring effective impedance matching and reliable performance.

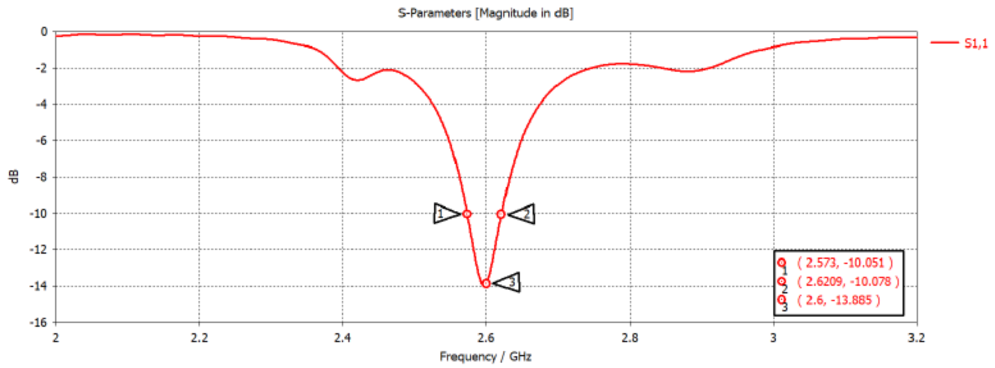

Figure 2. Return loss of eight cases with 32 holes.

Table 2. Configurations and radiation patterns of the antenna with 56 holes.

Case	Antenna configuration	Radiation pattern	Main beam direction
1	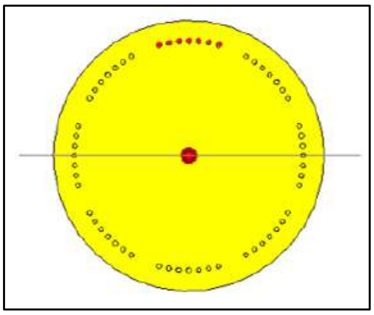	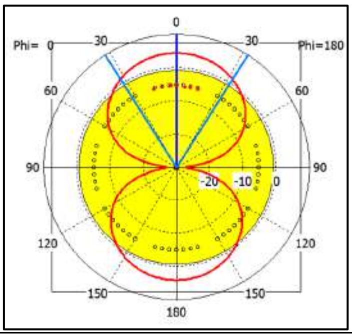	0˚
2	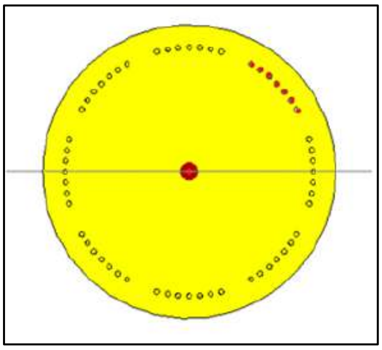	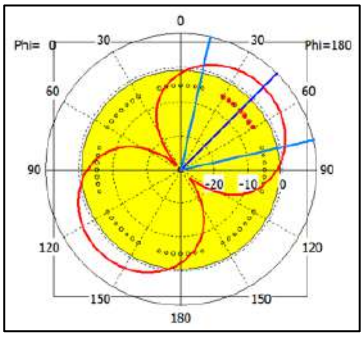	45˚
3	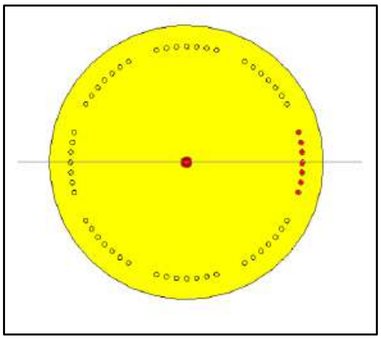	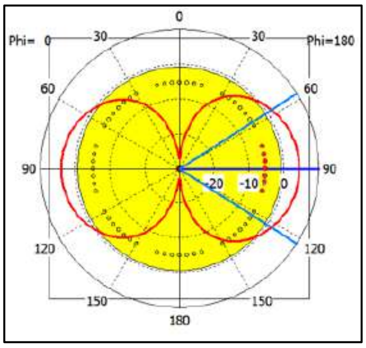	90˚
4	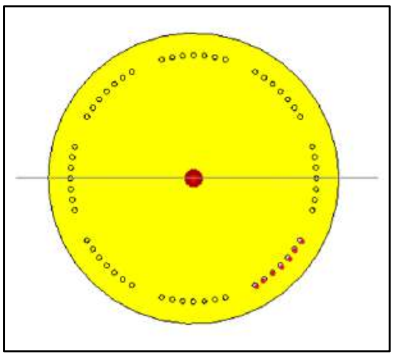	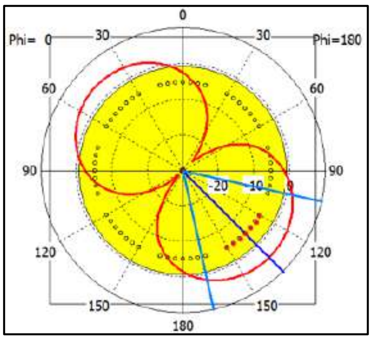	135˚

Table 2. Configurations and radiation patterns of the antenna with 56 holes. (Count.)

Case	Antenna configuration	Radiation pattern	Main beam direction
5	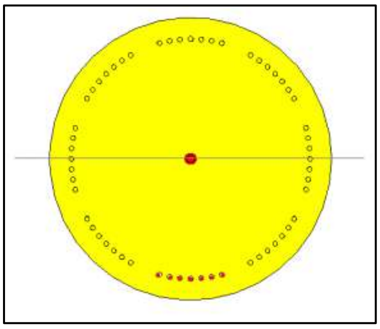	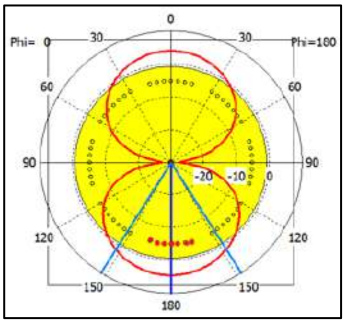	180˚
6	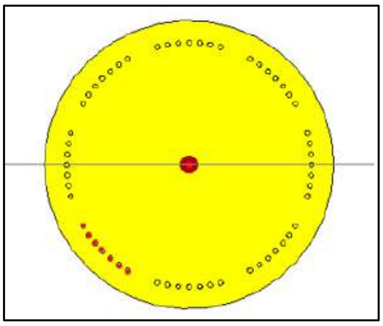	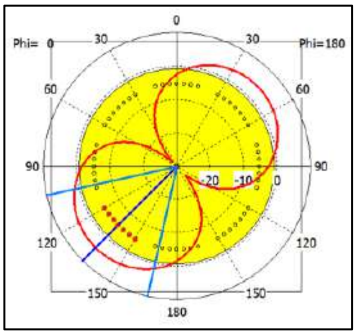	225˚
7	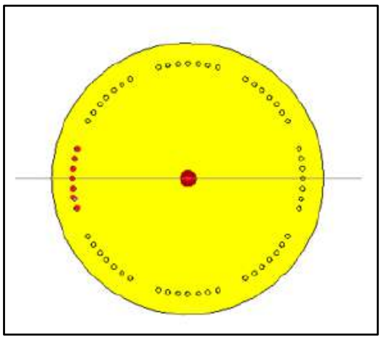	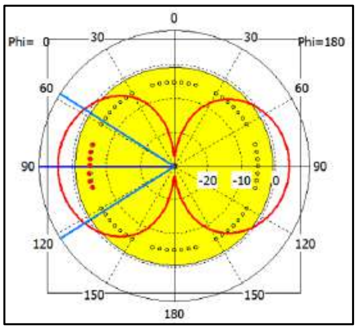	270˚
8	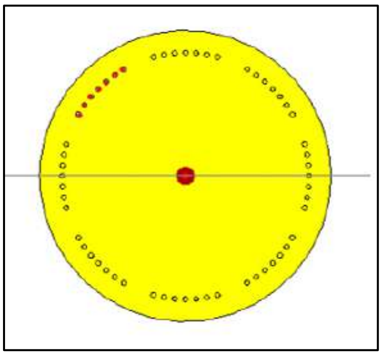	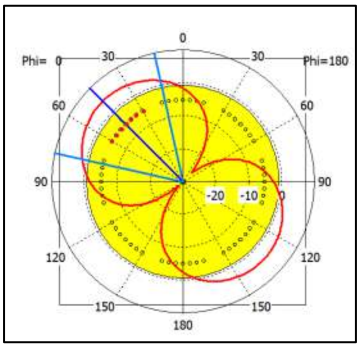	315˚

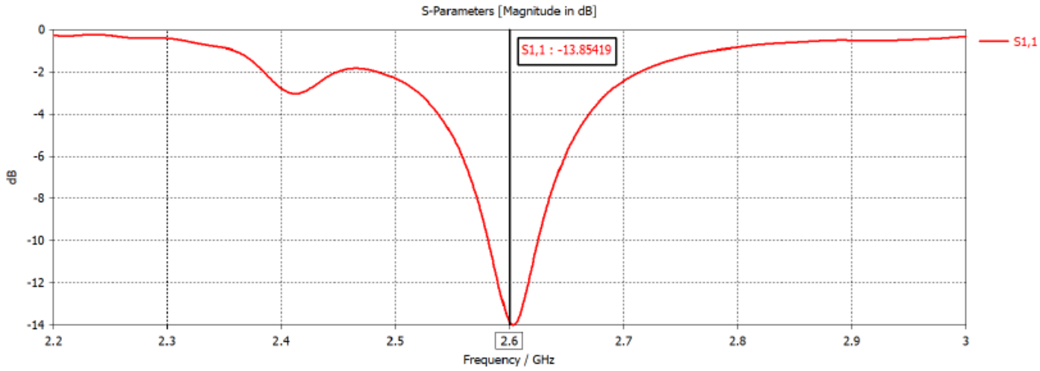

Figure 3. Return loss of eight cases with 56 holes.

shorted holes influence the current distribution and facilitate directional control. As shown in Figure 3 shows that the return loss across all eight configurations remains consistently acceptable, confirming that the antenna effectively operates at the desired frequency of 2.6 GHz. This stability is attributed to the symmetrical structure and balanced grouping of the short-circuited positions, ensuring effective impedance matching and reliable performance.

3. MACHINE LEARNING-BASED PREDICTION OF RETURN LOSS AND BEAM DIRECTION

To address the complexity of design parameters in circular microstrip antennas, ML techniques are employed to assist in predicting key antenna performance metrics. During the antenna design process, it was observed that multiple variables—such as hole positions, quantity, and spacing—can significantly affect performance. To efficiently manage this design variability, a dataset was generated using CST Studio Suite by simulating antenna configurations with drilled short-circuit holes along the inner edge of the circular patch.

Five different configurations were considered, comprising a uniform-spacing 32-hole configuration and non-uniform spacing configurations with 40, 56, 72, and 88 short-circuit holes. For each configuration, short-circuiting was applied to steer the main beam in eight distinct directions (0°, 45°, 90°, 135°, 180°, 225°, 270°, and 315°). The dataset includes input parameters and corresponding output values. The input parameters consist of:

(A) the open-circuiting direction (group number),
(B) the radial distance from the antenna center to the short-circuited position,
(C) the total number of shorted holes, and
(D) the spacing between shorted positions,

—as illustrated in Figure 4. For parameter (A), the short-circuiting direction is represented by group numbers ranging from 1 to 8, where each number corresponds to an open-circuit direction associated with the main beam direction: 1 = 0°, 2 = 45°, 3 = 90°, 4 = 135°, 5 = 180°, 6 = 225°, 7 = 270°, and 8 = 315°. The ML models are trained to predict two outputs: (X) the main beam direction (in degrees) and (Y) the return loss (in dB). For the antenna to operate effectively, the return loss must be greater than 10 dB (S_{11} less than -10 dB). Table 3 presents an example of 10 dataset entries, where all return loss values are within the acceptable range. Notably, one dataset exhibits a return loss of 9.4939332 dB, which is very close to the acceptable threshold of 10 dB. This indicates that even slight variations in design parameters can influence impedance matching. Additionally, the beam direction consistently aligns with the open circuit positions, validating the switching capability of the design. This approach streamlines the antenna design process, enabling efficient evaluation and optimization of multiple configurations without the need for extensive manual simulations.

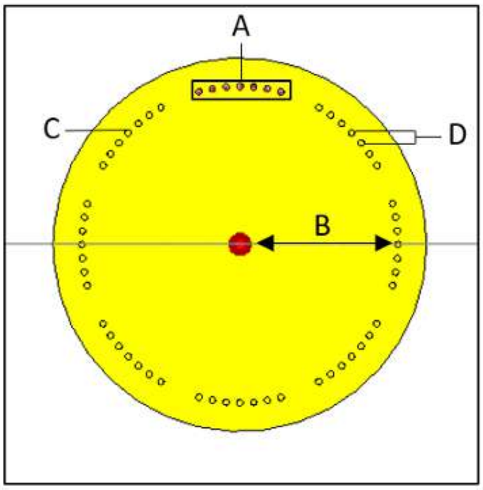

Figure 4. Prototype of a switched beam antenna with enhanced back lobe suppression.

Table 3. Machine Learning Prediction Results.

Input				Output									
				CST		Gradient Regression		Lasso Regression		Linear Regression		Random Forest	
A	B	C	D	X	Y	X	Y	X	Y	X	Y	X	Y
1	49	35	4	0	13.524858	0.1	13.65	0	12.91	0	13.33	0	12.82
2	49	63	4	45	13.970500	43.04	13.55	45	14.02	45	15.61	45	14.17
3	48	49	6	90	10.056579	90	16.48	90	15.23	90	15.18	90	12.08
4	51	35	6	135	14.256303	135	13.28	135	11.91	135	11.95	135	13.04
5	48.5	49	5	180	13.030897	180	14.10	180	14.52	180	14.40	180	13.72
6	49.5	35	5	225	9.4939332	225	13.92	225	13.15	225	13.18	225	13.35
7	50	49	4.5	270	11.955513	272.3	13.81	270	12.79	270	12.63	270	12.59
8	49.5	63	4.5	315	13.423955	314.89	11.93	315	13.63	315	13.21	315	12.83
6	49.5	63	4	225	13.398172	225	19.20	225	15.46	225	14.96	225	13.23
1	51	77	4	0	13.233036	0.1	14.09	0	12.06	0	12.08	0	13.94

To develop an effective machine learning-based prediction model, four algorithms were implemented: Gradient Regression, Lasso Regression, Linear Regression, and Random Forest. Since input and output values are continuous data that can vary over a range of numbers, regression methods are suitable for analyzing the relationship between input and output values. The implementation was conducted using Python, with a dataset generated from CST Studio Suite simulations. The collected data, consisting of 148 antenna design samples, was then used for model training and evaluation. The dataset enabled the algorithms to learn the relationship between input parameters and output values, with the models being trained to predict two key performance metrics: the main beam direction and the return loss.

Finally, the prediction accuracy of each algorithm was analyzed and compared to determine the most effective approach for optimizing antenna design. From Table 3, the prediction results show that Gradient Regression achieved an accuracy of 85.42%, Lasso Regression reached an accuracy of 63.56%, Linear Regression achieved an accuracy of 61.95%, and Random Forest demonstrated the highest accuracy at 99.39%. The radiation pattern has the main beam direction as designed in all cases and can operate at a frequency of 2.6 GHz. In the next section, a circular microstrip antenna capable of switching between 8 beam directions will be constructed, and the results will be measured.

4. EXPERIMENTAL VALIDATION AND COMPARISON OF FABRICATED ANTENNA WITH CST SIMULATIONS AND ML PREDICTIONS

In this section, we describe the fabrication of a circular microstrip antenna with a switched-beam mechanism, followed by performance measurements and comparisons with CST Studio Suite simulations and machine learning predictions. This validation aims to confirm that the fabricated antenna performs in accordance with both the simulation and prediction results.

The antenna is constructed on a substrate with a thickness (h) of 1.6 mm, a conductor and ground plane thickness of 0.03 mm, and overall dimensions of 110 mm × 110 mm. The dielectric constant of the substrate is 4.4. On the front side, a circular copper patch with a radius of 55.5 mm is implemented. A short-circuit mechanism is realized by inserting copper wires along 32 evenly spaced positions around the inner edge of the circular patch, as illustrated in Figure 5(a). On the back side, each hole position is equipped with a capacitor and a PIN diode, enabling control of the switching mechanism. Among the 32 positions, 28 are short-circuited in each configuration, while 4 remain open to direct the main beam. As shown in Figure 5(b), eight switching cases are realized:

Case 1 (yellow frame): Open circuit at 0°
Case 2 (pink frame): Open at 45°
Case 3 (green frame): Open at 90°
Case 4 (orange frame): Open at 135°
Case 5 (blue frame): Open at 180°
Case 6 (purple frame): Open at 225°
Case 7 (red frame): Open at 270°
Case 8 (black frame): Open at 315°

Finally, the antenna is connected with a stub and a microcontroller board to enable beam-switching control and to perform return loss and radiation pattern measurements, as shown in Figure 6.

After fabricating the antenna as designed, its performance was evaluated by measuring the return loss, radiation pattern, and antenna gain across all eight beam-switching configurations. For the antenna to be considered operational, the return loss must exceed 10 dB. Measurement results confirmed that the antenna operates effectively within the frequency range of 2.599 GHz to 2.631 GHz, successfully covering the target frequency of 2.6 GHz. The return loss at 2.6 GHz is 10.584 dB, with the highest measured value reaching 19.481 dB at 2.620 GHz, and an overall bandwidth of approximately 30–40 MHz. Since the return loss behavior is consistent across all eight switching cases, a single representative return loss plot is provided in Figure 7, confirming stable impedance matching and reliable frequency performance for the entire beam-switching system.

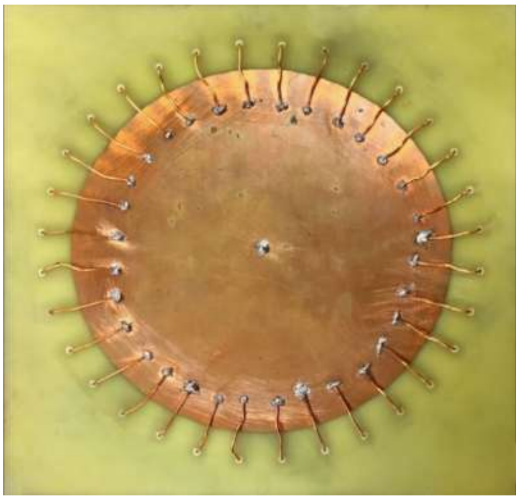

(a)

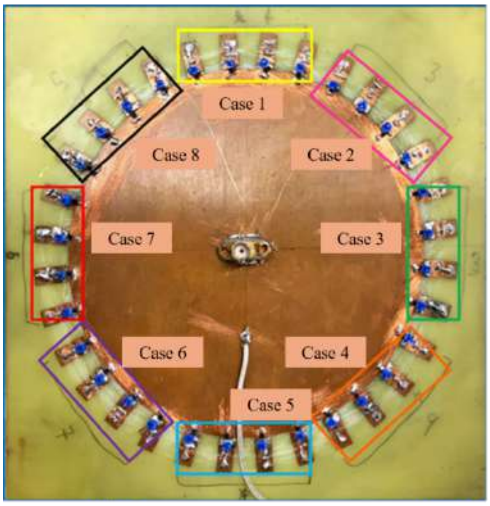

(b)

Figure 5. Fabricated antenna setup showing (a) top view with circular patch and (b) bottom view with switching components.

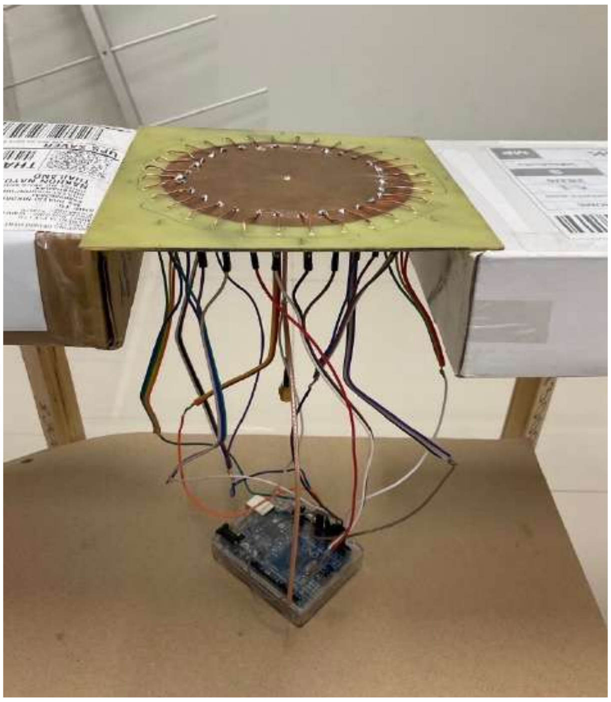

Figure 6. The antenna is connected to a stub and a microcontroller board.

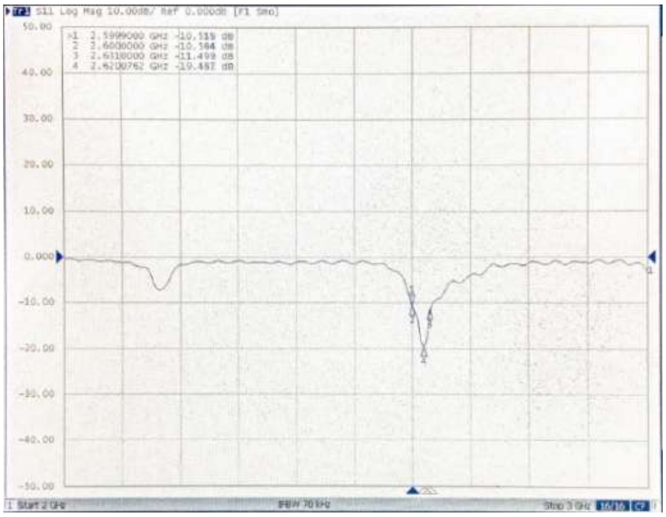

Figure 7. Return loss of the fabricated antenna.

The radiation pattern and antenna gain results for each case are as follows:
Case 1 (open circuit at the top side, 0°): Beam at 0°, gain of 10 dBi.
Case 2 (upper-right side, 45°): Beam at 50°, gain of 11 dBi.
Case 3 (right side, 90°): Beam at 65°, gain of 11 dBi.
Case 4 (lower-right side, 135°): Beam at 100°, gain of 9 dBi.
Case 5 (bottom side, 180°): Beam at 200°, gain of 7 dBi.
Case 6 (lower-left side, 225°): Beam at 230°, gain of 7 dBi.
Case 7 (left side, 270°): Beam at 275°, gain of 9 dBi.
Case 8 (upper-left side, 315°): Beam at 325°, gain of 9 dBi.

Although some measured main beam directions deviate slightly from the ideal design angles, the overall beam-switching trend remains consistent with CST simulation results, as shown in Table 4. These minor discrepancies are likely caused by environmental factors during measurement and the integration of the microcontroller circuit within the antenna structure. Additionally, the measured antenna gain varies slightly across cases, which may be attributed to these same influences, particularly the reduction in back lobe radiation introduced by the microcontroller. Despite these variations, the fabricated antenna demonstrates stable frequency performance and reliable beam-switching capability across all eight configurations. Importantly, the measurement results exhibit the same trend as both the CST simulation and machine learning predictions, as illustrated in Table 5.

Next, the transmitter position was randomized using a microcontroller-based control system. The control program was designed to randomly select an angle representing the transmitter's position, in order to test whether the antenna could correctly switch its beam direction in response. The beam-switching logic was defined based on angular sectors, as follows:

Case 1: If the transmitter position falls within 0°–22.5° or 337.5°–360°, the antenna switches its beam to 0°, as shown in Figure 8(a).

Case 2: For angles between 22.5°–67.5°, the beam is directed to 45°, as shown in Figure 8(b).

Case 3: For 67.5°–112.5°, the beam switches to 90°, as shown in Figure 8(c).

Case 4: For 112.5°–157.5°, the beam is directed to 135°, as shown in Figure 8(d).

Case 5: For 157.5°–202.5°, the beam switches to 180°, as shown in Figure 8(e).

Case 6: For 202.5°–247.5°, the beam is directed to 225°, as shown in Figure 8(f).

Case 7: For 247.5°–297.5°, the beam switches to 270°, as shown in Figure 8(g).

Case 8: For 297.5°–337.5°, the beam is directed to 315°, as shown in Figure 8(h).

Table 4. Comparison of simulated and measured radiation patterns

Case	Simulation results	Measurement results
1	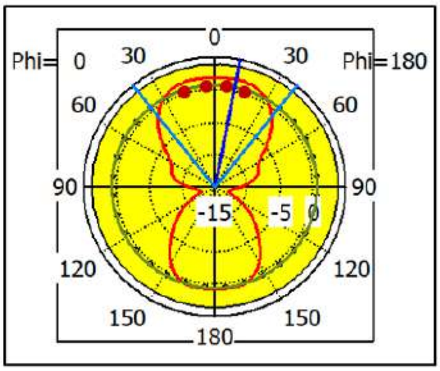	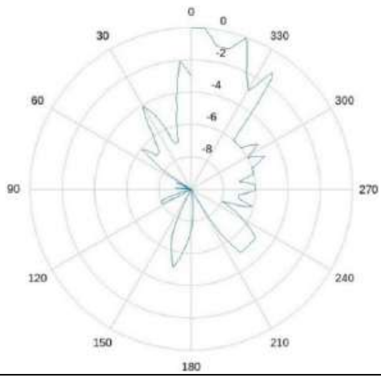
2	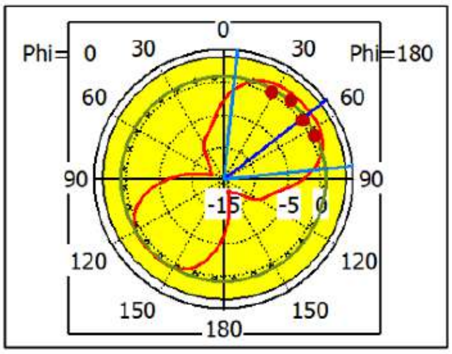	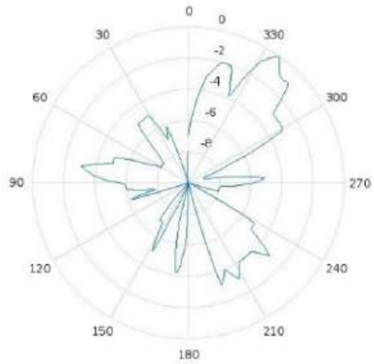
3	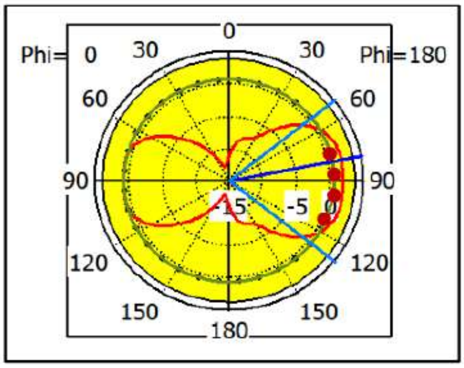	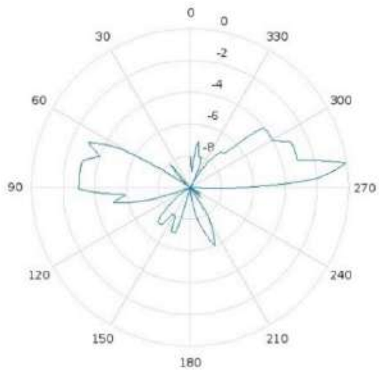

Table 4. Comparison of simulated and measured radiation patterns (Count.)

Case	Simulation results	Measurement results
4	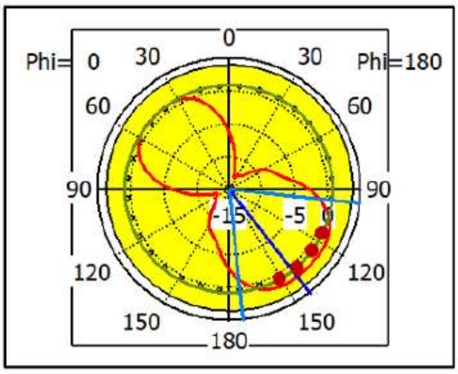	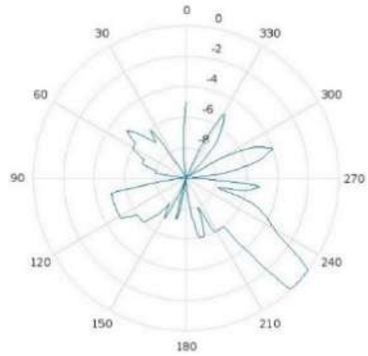
5	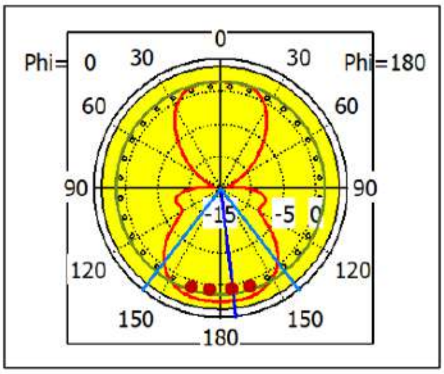	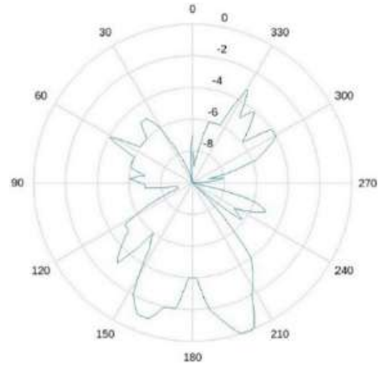
6	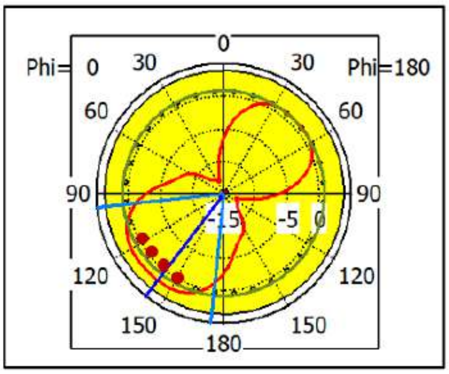	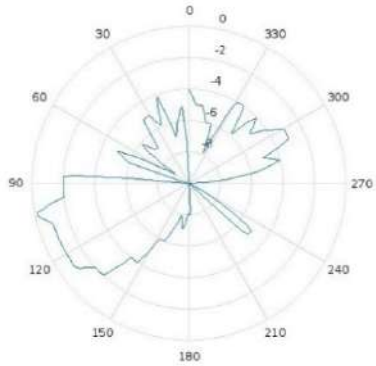
7	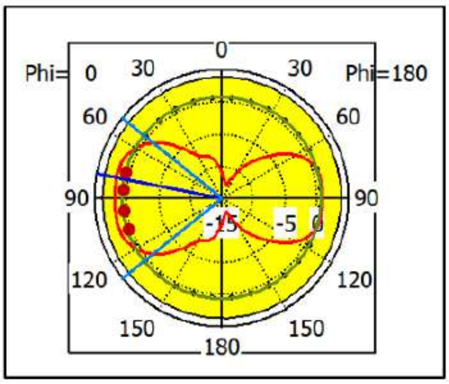	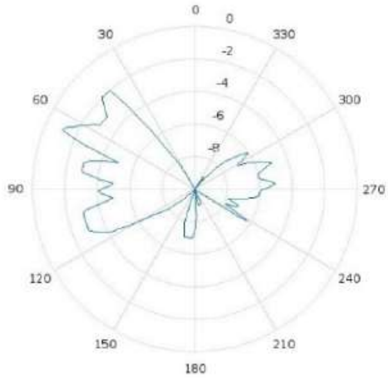

Table 4. Comparison of simulated and measured radiation patterns (Count.)

Case	Simulation results	Measurement results
8	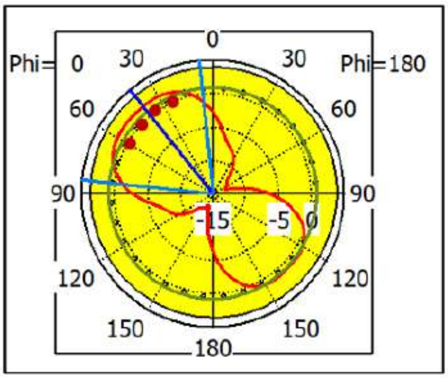	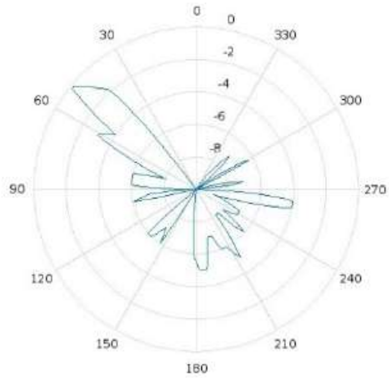

Table 5. Simulated, predicted, and measured performance of the antenna

CST		Random Forest		Measurement	
Main beam direction (degrees)	Return loss (dB)	Main beam direction (degrees)	Return loss (dB)	Main beam direction (degrees)	Return loss (dB)
0	13.524858	0	12.82	0	10.564
45	13.970500	45	14.17	50	10.139
90	10.056579	90	12.08	65	10.045
135	14.256303	135	13.04	100	10.321
180	13.030897	180	13.72	200	10.212
225	9.4939332	225	13.35	230	10.111
270	11.955513	270	12.59	275	10.352
315	13.423955	315	12.83	325	10.242

Upon testing all eight cases, the results confirmed that the beam direction was correctly selected based on the randomized input. Measurements of the radiation pattern further validated that the antenna successfully switched its main beam in accordance with the output from the microcontroller.

5. Conclusions

This paper presents the design, simulation, fabrication, and experimental validation of a 2.6 GHz single-element circular microstrip antenna with microcontroller-based 8-way beam-switching capability. The antenna was initially modeled in CST Microwave Studio based on calculated parameters. Eight beam-switching cases were defined to steer the main beam in the directions of 0°, 45°, 90°, 135°, 180°, 225°, 270°, and 315°, achieved by selectively shorting or opening circuit paths around the patch. Simulation results confirmed the antenna's ability to operate at 2.6 GHz, with the main beam steered correctly in all cases.

```
18:08:39.337 ->
18:08:40.311 -> output 0 angle
18:08:40.311 -> angle: 19.00
18:08:40.311 ->
```
(a)

```
18:08:01.298 ->
18:08:02.297 -> output 45 angle
18:08:02.297 -> angle: 42.00
18:08:02.297 ->
```
(b)

```
18:08:34.336 ->
18:08:35.326 -> output 90 angle
18:08:35.326 -> angle: 103.00
18:08:35.326 ->
```
(c)

```
18:08:49.358 ->
18:08:50.337 -> output 135 angle
18:08:50.337 -> angle: 147.00
18:08:50.337 ->
```
(d)

```
18:08:47.343 ->
18:08:48.330 -> output 180 angle
18:08:48.330 -> angle: 202.00
18:08:48.330 ->
```
(e)

```
18:09:04.352 ->
18:09:05.312 -> output 225 angle
18:09:05.312 -> angle: 240.00
18:09:05.358 ->
```
(f)

```
18:09:13.365 ->
18:09:14.354 -> output 270 angle
18:09:14.354 -> angle: 272.00
18:09:14.354 ->
```
(g)

```
18:09:16.337 ->
18:09:17.358 -> output 315 angle
18:09:17.358 -> angle: 318.00
18:09:17.358 ->
```
(h)

Figure 8. Beam-switching response of the antenna for randomized transmitter positions in (a) Case 1, (b) Case 2, (c) Case 3, (d) Case 4, (e) Case 5, (f) Case 6, (g) Case 7, and (h) Case 8, controlled by the microcontroller system.

To address the complex design parameter space involved in circular microstrip antennas, machine learning (ML) techniques were employed to predict key performance metrics, specifically return loss and beam direction. A dataset was generated using CST simulations, varying parameters such as the number of shorted holes, spacing, and position. Four regression-based ML models were trained: Gradient Regression, Lasso Regression, Linear Regression, and Random Forest. The Random Forest model achieved the highest accuracy at 99.39%, demonstrating excellent predictive capability for return loss and beam direction.

The antenna was fabricated on a double-sided 1.6 mm thick copper-clad substrate, with components such as capacitors, PIN diodes, an SMA connector, and a microcontroller interface integrated on the backside. A custom control program was developed for the microcontroller to automate beam-switching based on the angular position of the transmitter, mimicking real-world adaptive beam-steering behavior.

Comparative analysis among CST simulations, Random Forest ML predictions, and measurement results confirms that the antenna consistently operates near 2.6 GHz, with beam directions exhibiting the same switching trend across all cases. Although minor discrepancies were observed in the measured main beam angles—attributable to environmental conditions and hardware integration—the antenna's performance remains robust. The return loss in all configurations exceeds 10 dB, validating the design's impedance matching.

Therefore, the proposed antenna demonstrates energy-efficient and reliable 8-way beam switching, supported by both simulation and data-driven ML prediction. The integration of a microcontroller system enables real-time directional control, making this antenna a promising candidate for 5G and next-generation wireless communication systems.

Conflicts of Interest: The authors declare no conflict of interest.

Funding

This work was supported by Srinakharinwirot University (SWU) and Faculty of Engineering, SWU, Thailand through the research grant No. 197/2567.

Acknowledgments

This work was supported by Srinakharinwirot University (SWU) and Faculty of Engineering, SWU, Thailand.

Declaration of generative AI and AI-assisted technologies in the writing process

During the preparation of this work, the authors used AI-assisted technologies to improve only language and readability. After using this tool/service, the authors reviewed and edited the content as needed and takes full responsibility for the content of the publication.

Data availability statements: The datasets used and/or analyzed during the current study available from the corresponding author on reasonable request.

References

[1] Denis, A. (2019). Overview of ITU-T Activities on 5G/IMT-2020. *in ITU Committed to Connecting the World*, [Online]. Available: https://www.itu.int

[2] Sanou, B. (2017). Setting the Scene for 5G: Opportunities & Challenges. *in 2018 International Telecommunication Union*, [Online]. Available: https://www.itu.int

[3] Lee, C. (2017). 5G Basics, in *2017 International Telecommunication Union*, [Online]. Available: https://www.itu.int

[4] Carugi, M. (2018). Key Features and Requirements of 5G/IMT-2020 Networks. *in 2018 ITU Arab Forum on Emerging Technologies*, [Online]. Available: https://www.itu.int

[5] Nordrum A. and Clark, K. (2019). Everything You Need to Know About 5G. *IEEE Spectrum: Technology, Engineering, and Science News*, Oct. 2019.

[6] Gross Frank, B. (2005). Smart antenna, in Smart Antenna for Wireless Communications with MATLAB. *1st ed., McGraw-Hill*, 207–266.

[7] Zooghby, A. E. (2005). Fixed beam smart antenna systems and adaptive array systems. *in Smart Antenna Engineering*, *Artech House Publishers*, 83–158.

[8] Zahar, Z. and Bin Ain, M. F. (2022). Backlobe reduction of air substrate circular patch antenna for 5G applications. *11th International Conference*

on Robotics, Vision, Signal Processing and Power Applications, Feb, 948–954.

[9] Wang, D., Wei, X. , Zhang, J., Shu, Y. and Yang, D. (2015). Back lobe reduction of patch antenna by using high-impedance surface (Invited). *IET International Radar Conference 2015*, Hangzhou, 1–4.

[10] Ali, M. T., Rahman, T. A., Kamarudin, M. R., Sauleau, R., Tan, M. N. M. and Jamlos, M. F. (2010). A Reconfigurable Planar Antenna Array (RPAA) with back lobe reduction. *2010 International Workshop on Antenna Technology (iWAT),* Lisbon, Portugal, 1-4.

[11] Liu, R., Ma, K., Yan, N., Wang, Y. and Wu, Y. (2024). An FR4-Based Miniaturized High-Efficiency Double-Sided SISL Longitudinal Slot Antenna Array for 5G Millimeter-Wave Applications. *in IEEE Transactions on Antennas and Propagation*, 72(7), 6099-6104.

[12] Singh, U. and Mishra, R. (2022). A Dual-Band High-Gain Substrate Integrated Waveguide Slot Antenna for 5G Application. *Progress In Electromagnetics Research C*, 119, 191-200.

[13] Rana, M. S., Islam, S. M. R. and Sarker, S. (2024). Machine learning based on patch antenna design and optimization for 5 G applications at 28GHz. *Results in Engineering*, 24, 1-14.

[14] Pandey, A. K., Singh, M. P. (2023). Antenna Optimization using Machine Learning Algorithms and their Applications: A Review. *Journal of Engineering Science and Technology Review*, 17(2), 128-144.

[15] Haque, M.A., Rahman, M.A., Al-Bawri, S.S., et al. (2023). Machine learning-based technique for gain and resonance prediction of mid band 5G Yagi antenna. *Sci Rep*, 13(12590), 1-22.

[16] Zhong, Y., Renner, P., Dou, W., Ye, G., Zhu, J. and Liu, Q. H. (2022). A Machine Learning Generative Method for Automating Antenna Design and Optimization. *arXiv*, 1-16.

[17] Zhong, Y., Renner, P., Dou, W., Ye, G., Zhu, J. and Liu, Q. H. (2022). A Machine Learning Generative Method for Automating Antenna Design and Optimization. *in IEEE Journal on Multiscale and Multiphysics Computational Techniques*, 7, 285-295.

[18] Haque, M. A., Rahman, M. A., Al-Bawri, S. S., Yusof, Z., Sharker, A. H., Abdulkawi, W. M., Saha, D., Paul, L. C. and Zakariya, M. A. (2023). Machine Learning-based Technique for Gain and Resonance Prediction of Mid Band 5G Yagi Antenna. *Scientifc Reports*, 13(12590), 1-22.

[19] Sarker, N., Podder, P., Mondal, M. R. H., Shafin, S. S. and Kamruzzaman, J. (2023). Applications of Machine Learning and Deep Learning in Antenna Design, Optimization, and Selection: A Review. *in IEEE Access*, 11, 103890-103915.

[20] Sharma, K. and Pandey, G. P. (2021). Efficient modelling of compact microstrip antenna using machine learning. *AEU - International Journal of Electronics and Communications*, 135, 1-13.

[21] Haque, M. A., Sarker, N., Sawaran Singh, N. S., Rahman, M. A., Hasan, M. N., Islam, M., Zakariya, M. A., Paul, L. C., Sharker, A. H., Abro, G. E. M., Hannan, M. and Pk, R. (2022) Dual Band Antenna Design and

Prediction of Resonance Frequency Using Machine Learning Approaches. *Applied Sciences*, 12(10505), 1-18.

[22] Jain, R., Ranjan, P., Singhal, P. K. and Thakare, V. V. (2022). Estimation of S11 Values of Patch Antenna Using Various Machine Learning Models. *2022 IEEE Conference on Interdisciplinary Approaches in Technology and Management for Social Innovation (IATMSI)*, Gwalior, India, 1-4.

[23] Mahmoud, K. R. and Montaser, A. M. (2022). Machine-learning-based beam steering in a hybrid plasmonic nano-antenna array. *Journal of the Optical Society of America B*, 39(8), 2149-2163.

[24] Montaser, A. M. and Mahmoud, K. R. (2021). Deep Learning Based Antenna Design and Beam-Steering Capabilities for Millimeter-Wave Applications. *in IEEE Access*, 9, 145583-145591.

[25] Fakharian, M. M. (2025). Machine learning approach for evaluation of beam-string in a metasurface-based terahertz antenna for 6G networks. *Materials Today Communications*, 43, 2025.

[26] Noimi, W. and Chaipanya, P. (2024). Wide-band Circular Slot Antenna Beam Switching Directions Using Machine Learning Algorithms. *2024 IEEE Asia Pacific Conference on Circuits and Systems (APCCAS)*, Taipei, Taiwan, 484-488.

[27] Nikornpon, O. and Chaipanya, P. (2024). Predicting Beam Switching Directions in Ultra Wideband Spiral Antennas Using Machine Learning Algorithms. *2024 IEEE Asia Pacific Conference on Circuits and Systems (APCCAS)*, Taipei, Taiwan, 479-483.

[28] Balanis, C. A. (2015). Antenna. Theory. Analysis and Design (3rd. Edition). *A John Wiley & Sons, Inc., Publication*.